Dynamics of the formation of the self-trapped exciton in the MX complex PtBr(en)

4 AUTHORS, INCLUDING:

Aaron D. Van Pelt
Picarro

39 PUBLICATIONS   **236** CITATIONS

James Brozik
Washington State University

48 PUBLICATIONS   **592** CITATIONS

Dynamics of the formation of the self-trapped exciton in the MX complex PtBr(en)

S.L. Dexheimer[a,*], A.D. Van Pelt[a], J.A. Brozik[b], B.I. Swanson[b]

[a]*Department of Physics, Washington State University, Pullman, WA, USA*
[b]*Chemical Sciences and Technology Division, Los Alamos National Laboratory, Los Alamos, CA, USA*

Abstract

We have directly time-resolved the coupled electronic and vibrational dynamics of the self-trapping process in a quasi-one-dimensional system, the halide-bridged mixed-valence transition metal linear chain (MX) complex $[Pt(en)_2][Pt(en)_2Br_2]\cdot(PF_6)_4$, (en: ethylenediamine, $C_2H_8N_2$) using femtosecond spectroscopic techniques in the vibrationally impulsive limit. In these experiments, we impulsively excite the optical intervalence charge-transfer transition with light pulses 35 fs in duration, short compared to the period of the characteristic chain-axis vibrational motion. The red-shifted absorbance of the self-trapped exciton state, which forms on a time scale of $\sim$200 fs, is modulated by vibrational wavepacket oscillations that correspond to lattice motions induced by the optical excitation. In addition to detecting an oscillatory response consistent with impulsive stimulated Raman excitation of the ground-state symmetric chain-axis stretching mode at $\sim$175 cm^{-1}, and its harmonics, we find that the self-trapped exciton absorbance is strongly modulated by a heavily damped, low frequency wavepacket component at $\sim$110 cm^{-1}. The coherence time of this new frequency component closely parallels the induction of the self-trapped exciton absorbance, consistent with a wavepacket corresponding to the lattice motion that carries the excited system to the self-trapped state. The spectral evolution of the low-frequency wavepacket oscillation provides a detailed picture of the coupled electron-lattice dynamics of the photo-excited state. © 2001 Elsevier Science B.V. All rights reserved.

Keywords: Time-resolved fast spectroscopy; Photo-induced absorption spectroscopy

The halogen-bridged mixed-valence transitional metal chain, or MX, complexes are useful model systems for investigating the physics of quasi-one-dimensional solids [1,2]. In particular, the vibrational characteristics as well as the structural tunability of these complexes make them ideal for studying the coupled electron-lattice dynamics that drive the formation of the self-trapped exciton. In this process, an electronic excitation is stabilized by a self-induced local lattice distortion, resulting in a localized state, the self-trapped exciton, which is generally the primary photo-excitation in quasi-one-dimensional systems. Despite its fundamental importance, a clear observation of the dynamics of the self-trapping in quasi-one-dimensional systems has proved elusive prior to this work [3,4].

A simplified diagram of the quasi-one-dimensional structure of an MX complex is shown in Fig. 1a, which shows both the periodic charge disproportionation (or mixed-valence character) and the periodic bond length distortion (or Peierls distortion) characteristic of the charge density wave ground state. Not shown in this simplified structure are

the ethylenediamine ligands, which fill the transverse bonding sites on the octahedrally coordinated metal ions, or the PF_6 counterions, which serve to balance the overall charge in the crystal structure, as well as to spatially separate the chains so that they experience minimal interchain interaction. An important aspect of the utility of the MX materials as model systems lies in their chemical tunability: for example, the bridging halide has a profound effect on the strength of the electron–phonon coupling, and with it, the strength of the charge density wave state. As the halide X in the platinum complexes is varied through the series Cl, Br, and I, the strength of the electron–phonon interaction varies from very strong coupling in the highly distorted, valence-localized PtCl system to much weaker coupling in the valence-delocalized PtI system.

The optical absorption spectrum of the MX complexes is dominated by the optical intervalence charge transfer transition (IVCT), a strongly polarized electric dipole transition that effectively transfers charge between inequivalent metal sites, as shown schematically in Fig. 1b. Since the equilibrium metal-halide bond lengths depend on the charge distribution about the metal ions, the IVCT transition is strongly coupled to the Raman-active symmetric stretching

---

... -------X⁻-- Pt$^{+(3+\delta)}$--X⁻------- Pt$^{+(3-\delta)}$-------X⁻-- Pt$^{+(3+\delta)}$--X⁻------- Pt$^{+(3-\delta)}$------- ...

(a) charge density wave ground state

... -------X⁻-- Pt$^{+(3+\delta)}$--X⁻------- Pt$^{+(3-\delta)}$-------X⁻-- Pt$^{+(3+\delta)}$--X⁻------- Pt$^{+(3-\delta)}$------- ...

(b) optical intervalence charge-transfer transition

... -------X⁻-- Pt$^{+(3+\delta)}$--- X⁻ ---- Pt^{+3} ---- X⁻ ---- Pt^{+3} ---- X⁻ ------- Pt$^{+(3-\delta)}$------- ...
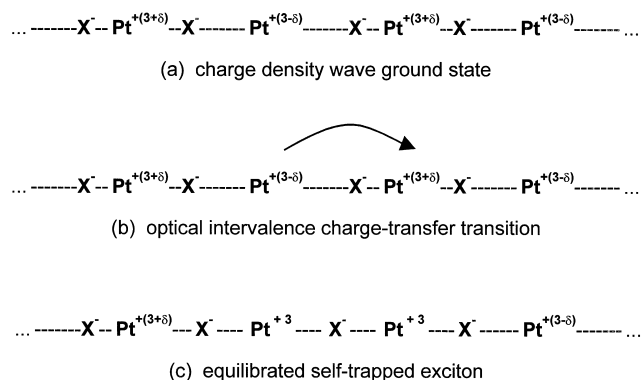
(c) equilibrated self-trapped exciton

Fig. 1. Schematic structure of the linear chain-axis of an MX complex, showing (a) the charge density wave ground state, with alternating valence states on the Pt ions and corresponding distortions in the metal-halide bond lengths, (b) the optical IVCT, which effectively transfers charge between inequivalent metal sites, and (c) a schematic representation of the self-trapped exciton state.

mode (ν_1). Excitation of the IVCT band creates a highly nonequilibrium lattice configuration that subsequently relaxes to form localized nonlinear excitations, and generation of self-trapped excitons together with their decay into solitons and polarons have been predicted theoretically using Peierls–Hubbard models [1,5–7]. The schematic structure of the self-trapped exciton state is shown in Fig. 1c. For the purposes of illustration, the self-trapped exciton in this figure is represented by two adjacent M^{3+} ions, although the actual spatial extent of the localized excitation may be larger, depending on the strength of the electron-lattice interaction in a particular material.

Since self-trapping in an ideal one-dimensional system is expected to be a barrierless process (in contrast to three-dimensional systems where, in general, there is an adiabatic potential barrier between the free and self-trapped states) [8], the formation time for the self-trapped exciton is expected to be extremely fast. Previous experimental work on metal-halide complexes similar to that used in the current study indicates that the dynamics are rapid: luminescence measurements on PtCl complexes indicate a large Stokes shift as well as sub-picosecond to picosecond luminescence lifetimes that have been attributed to cooling and decay of the self-trapped exciton state [9–12]. In addition, transient absorption measurements have revealed a red-shifted induced absorbance assigned to the self-trapped exciton state that decays on a picosecond time scale [13,14]. The initial relaxation processes leading to the formation of the self-trapped exciton are thought to occur on a femtosecond time scale, consistent with the idea that the chain-axis vibrational modes directly drive this process.

The vibrational properties of MX complexes have been characterized by Raman and far-infrared spectroscopies [15,16]. The vibrational spectra of the complexes have been interpreted in detail, and reveal strong modes involving motions along the chain-axis. In PtBr complexes, these include a Raman-active symmetric stretch of the Br ions

about the Pt ions at a frequency of $\sim$180 cm^{-1}, corresponding to a period of 185 fs, an infrared-active asymmetric stretch at $\sim$240 cm^{-1}, and a lower frequency infrared-active mode at $\sim$95 cm^{-1}. The relatively slow chain-axis vibrational motions of the MX complexes (in contrast to, for example, the much faster carbon–carbon stretching modes in organic conjugated conducting polymers) make it possible to clearly time-resolve the vibrational dynamics associated with the self-trapping process, as seen in the measurements below.

Femtosecond pump-probe measurements were carried out on single crystals of [Pt(en)$_2$][Pt(en)$_2$Br$_2$]·(PF$_6$)$_4$. Recent advances in the synthesis of the MX complexes have resulted in materials that are largely free of defects and that are resistant to photo-induced damage [17]. To resolve the vibrational dynamics in these measurements, we have used femtosecond spectroscopic techniques in the vibrationally impulsive limit [18,19]. Fig. 2 shows the time-resolved differential transmittance following excitation of the IVCT transition with light pulses 35 fs in duration, short compared to the period of the characteristic chain-axis vibrational motion. The response was measured using a degenerate pump-probe configuration, in which identical pulses are used for the pump and the probe [4]. As can be seen in the figure, the time-resolved response is modulated by large-amplitude wavepacket oscillations. Underlying the oscillations is an induced absorbance signal that forms on a time scale of $\sim$200 fs and corresponds to the red-shifted absorption of the self-trapped exciton state. The frequency content of the oscillations is evident in the Fourier power spectrum in the inset of Fig. 2, which shows a large component at 175 cm^{-1}, corresponding to the frequency of the Raman-active symmetric stretching mode in the ground state of the
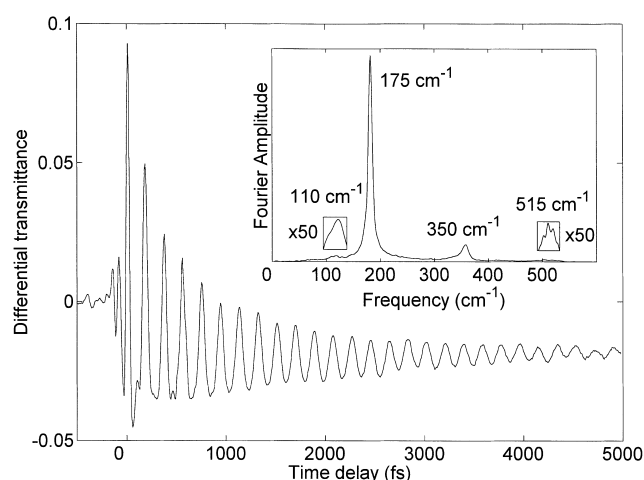
Fig. 2. Time-resolved differential transmittance of the [Pt(en)$_2$][Pt(en)$_2$Br$_2$]·(PF$_6$)$_4$ complex following excitation of the optical IVCT with pulses 35 fs in duration centered at 800 nm, near the onset of the IVCT. The response was measured in the degenerate pump-probe configuration, and the component of the transmitted probe pulse at 830 nm was detected. The Fourier power spectrum of the oscillatory part of the data trace is shown in the inset.

complex. Additional components are present at the second and third harmonics; these are also apparent in the resonance Raman spectrum, consistent with the strong electron–phonon coupling for this mode. It is important to note that, even though the 830 nm detection wavelength lies within the absorption spectrum of the self-trapped exciton (as evidenced by the induced absorbance), the vibrational response in Fig. 2 is dominated by wavepacket oscillations at the ground state vibrational frequencies. This response is consistent with excitation of the ground state vibrational wavepackets by the impulsive stimulated Raman scattering process [20,21], which is resonantly enhanced by pumping the IVCT, to which the vibrational mode is strongly coupled. A weak component at 110 cm^{-1} is also apparent in the Fourier spectrum. This frequency is not present in the Raman spectrum, and is assigned to an excited state wavepacket using the additional measurements presented below.

To more clearly observe the dynamics associated with the formation of the self-trapped exciton, it is necessary to probe at detection wavelengths farther away from the IVCT transition, and farther into the red-shifted absorption band of the self-trapped exciton. The differential transmittance at a detection wavelength of 880 nm, measured using a femtosecond white-light continuum, is shown in Fig. 3. This signal shows a large induced absorbance corresponding to the self-trapped exciton population that forms on a time scale of ~200 fs and decays on a time scale of several picoseconds [4]. The signal is again modulated by wavepacket oscillations that include a strongly damped component at 110 cm^{-1} in addition to a component corresponding to the Raman-active ground state symmetric stretch mode at 175 cm^{-1}.

The dynamics of the strongly damped 110 cm^{-1} component are evident in Fig. 4a, which shows the differential transmittance at a series of detection wavelengths starting in the Franck–Condon region at 830 nm and extending far into the self-trapped exciton absorption spectrum. Fig. 4b shows

Fig. 4. (a) Time-resolved differential transmittance of PtBr(en), measured using a femtosecond white light continuum probe, at a series of detection wavelengths: 830, 855, 905, and 940 nm. (b) The strongly damped low-frequency oscillatory component extracted by LPSVD analysis from each data trace, showing the phase evolution of the excited state wavepacket.

the 110 cm^{-1} component extracted from each data trace using linear prediction/singular value decomposition (LPSVD) methods. The dephasing time of this frequency component closely parallels the induction of the self-trapped exciton absorbance, consistent with a wavepacket corresponding to the lattice motion that carries the excited system to the self-trapped state [3]. The phase evolution of the wavepacket response with detection wavelength provides a detailed picture of the wavepacket dynamics. Perhaps most striking is the observation that, although self-trapping is expected to be a rapid, barrierless process, the wavepacket evolution in the excited state exhibits clear recurrences.

We note that the vibrational characteristics of the MX complexes (the relatively slow vibrations and the simple one-dimensional mode structure) have made it possible to clearly time-resolve the excited state trapping dynamics. Even with these favorable characteristics, it is still necessary to carefully distinguish between the excited state wavepacket response and the large amplitude ground state vibrational response that results from impulsive excitation of the strongly Raman-active symmetric mode. Even though the excitation pulse duration in this experiment is less than one-fifth the duration of the ground state vibrational frequency, substantial Raman excitation can still occur, and can produce a modulation of the differential transmittance at wavelengths well to the red of the excited transition. This behavior is consistent with the impulsive stimulated Raman excitation mechanism [18–21]. It appears likely that impulsive excitation experiments on organic conjugated conducting polymers, which have strongly Raman-active ground state vibrational modes with periods of ~16–20 fs, will yield responses dominated by ground state impulsive Raman processes, especially when probed near the Franck–Condon
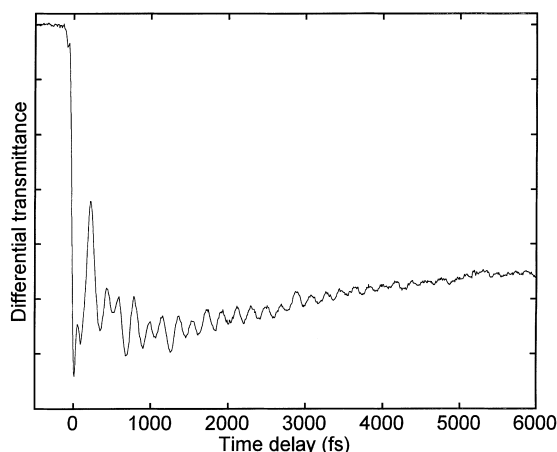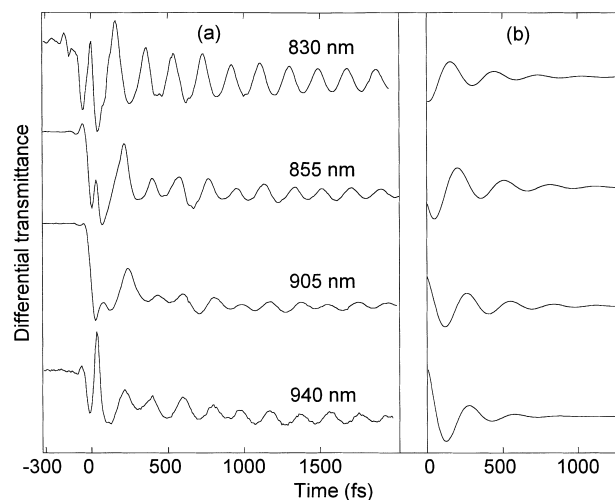

Fig. 3. Time-resolved differential transmittance of PtBr(en) measured in the continuum probe configuration, with a detection wavelength of 880 nm, well within the red-shifted absorption band of the self-trapped exciton state.

region. This is consistent with a number of recent experimental results on conjugated polymer systems that show oscillatory modulation only at frequencies present in the cw Raman spectrum, even when the excitation and probe pulses are as short as 5 fs.

In conclusion, we have directly time-resolved the vibrational dynamics associated with the self-trapping process in a quasi-one-dimensional system by carrying out femtosecond impulsive excitation measurements on the PtBr(en) complex. Moreover, the structural tunability of the MX complexes allows the self-trapping dynamics to be studied directly as a function of the strength of the electron–phonon interaction, as seen in our forthcoming work on the PtCl(en) complex.

Acknowledgements

References

[1] J.T. Gammel, et al., Phys. Rev. B 45 (1992) 6408.
[2] B. Scott, et al., J. Mol. Struct. 356 (1995) 207.
[3] S.L. Dexheimer, et al., Phys. Rev. Lett. 84 (2000) 4425.
[4] S.L. Dexheimer, et al., J. Phys. Chem. A 104 (2000) 4308.
[5] M. Suzuki, K. Nasu, Phys. Rev. B 45 (1992) 1605.
[6] A. Mishima, K. Nasu, Phys. Rev. B 39 (1989) 5758.
[7] A. Mishima, K. Nasu, Phys. Rev. B 39 (1989) 5763.
[8] K.S. Song, R.T. Williams, Self-Trapped Excitons, 2nd Edition, Springer Series in Solid-State Sciences, Vol. 105, Springer, New York, 1996.
[9] S. Tomimoto, et al., Phys. Rev. Lett. 81 (1998) 417.
[10] Y. Wada, et al., J. Lumin. 58 (1994) 146.
[11] Y. Wada, K. Era, M. Yamashita, Solid State Commun. 67 (1988) 953.
[12] H. Tanino, W.W. Ruhle, K. Takahashi, Phys. Rev. B 38 (1988) 12716.
[13] H. Ooi, M. Yamashita, T. Kobayashi, Solid State Commun. 86 (1993) 789.
[14] G.S. Kanner, et al., Phys. Rev. B 56 (1997) 2501.
[15] R.J.H. Clark, in: R.J.H. Clark, R.E. Hester (Eds.), Advances in Infrared and Raman Spectroscopy, Wiley, New York, 1984, p. 95.
[16] S.P. Love, et al., Phys. Rev. B 47 (1993) 11107, and references therein.
[17] J.A. Brozik, et al., Inorg. Chem. Acta 294 (1999) 275.
[18] L. Dhar, J.A. Rogers, K.A. Nelson, Chem. Rev. 94 (1994) 157.
[19] W.T. Pollard, S.-Y. Lee, R.A. Mathies, J. Chem. Phys. 92 (1990) 4012.
[20] S.L. Dexheimer, et al., Chem. Phys. Lett. 188 (1992) 61.
[21] W.T. Pollard, et al., J. Phys. Chem. 96 (1992) 6147.